The object of this study is the grinding process in a tumbling mill when the mechanism of destruction by abrasion is implemented, which is caused by the mechanism of shear loading. The abrasive effect due to the impulse interaction during the mutual chaotic movement of granular particles in the shear layer of loading, characterized by the granular temperature, is taken into account.

The task solved was determining the parameters of the shear interaction, which is caused by the difficulties of modeling and complexity of the hardware analysis of behavior of the internal loading in the mill.

A mathematical model was built based on data visualization for the abrasion grinding mechanism.

The power of the shear interaction forces was taken as an analog of the grinding performance. The initial shear characteristic was considered to be the average value of the shear velocity gradient in the central averaged normal section of the shear layer. The impact on productivity of the granular temperature and mass fraction of the shear layer and loading turnover was taken into account.

The effect of rotation speed on performance was evaluated by experimental modeling at a chamber filling degree of 0.45 and a relative particle size of 0.0104. The maximum value of the energy and productivity of grinding by abrasion was established at the relative speed of rotation ψ_ω=0.55–0.6.

The results have made it possible to establish a rational speed when grinding by abrasion, ψ_ω=0.5–0.6. This value is smaller in comparison with grinding by crushing ψ_ω=0.55–0.65 and breaking ψ_ω=0.75–0.9. The established effect is explained by the detected activation of the chaotic quasi-thermodynamic movement of particles of the shear layer at slow rotation.

The model built makes it possible to predict rational technological parameters of the energy-saving process of fine grinding in a tumbling mill by abrasion

Keywords: tumbling mill, intra-chamber loading, grinding by abrasion, granular temperature, grinding performance

UDC 621.926.5:539.215
DOI: 10.15587/1729-4061.2024.301653

BUILDING A MODEL OF THE ABRASION GRINDING MECHANISM IN A TUMBLING MILL BASED ON DATA VISUALIZATION

Yuriy Naumenko
Corresponding author
Doctor of Technical Sciences,
Associate Professor, Professor
Department of Construction, Road
and Reclamation Machines*
E-mail: informal9m@i.ua
Kateryna Deineka
PhD, Teacher of the Highest Category
Rivne Technical Vocational College*
Serhii Zabchyk
Institute of Mechanical Engineering*
*National University of Water
and Environmental Engineering
Soborna str., 11, Rivne, Ukraine, 33028

Received date 16.01.2024
Accepted date 05.04.2024
Published date 30.04.2024

How to Cite: *Naumenko, Y., Deineka, K., Zabchyk, S. (2024). Building a model of the abrasion grinding mechanism in a tumbling mill based on data visualization. Eastern-European Journal of Enterprise Technologies, 2 (1 (128)), 21–33. https://doi.org/10.15587/1729-4061.2024.301653*

1. Introduction

Grinding in tumbling mills is a rather energy-intensive process due to the dissipation of energy during the shear circulation of the internal chamber loading [1]. Reducing the energy intensity of the work processes of these disintegrators remains a relevant issue [2].

The task of modeling and forecasting the energy consumption of tumbling mills was solved by various methods, which turned out to be quite contradictory. The resulting models do not make it possible to establish a relationship between the power of the drive and the productivity of the grinding process [3].

One of the main load mechanisms during grinding in tumbling mills, in addition to impact and compression, is shear [4]. This load causes tangential stresses and surface friction between grinding bodies and particles of the crushed material [5]. Shear loading enables the implementation of an abrasion destruction mechanism [4, 6, 7] mainly in the surface layer of the material particle during fine grinding [8]. The implementation of the specified mechanisms is carried out in the zone of shear movement of granular intra-chamber loading (Fig. 1) [5, 9].

A significant part of tumbling mills carries out fine grinding due to a significant part of the impact on the grinding of the mechanism of destruction by abrasion during shear loading. However, the determination of shear interaction parameters is quite problematic because of the insurmountable difficulties of analytical and numerical modeling and the increased complexity of hardware analysis of loading pattern.

The granular temperature is a physical phenomenological parameter that roughly determines the energy of mutual movements of the particles of a sheared granular layer. A number of proven methods of analytical and experimental determination of the granular temperature of shear gravity granular flows were devised. They are widely used to model individual qualitative characteristics of the behavior of the shear layer of the intra-chamber granular loading of a rotating drum.

However, the quantitative results of the impact of the shear action on grinding remain unknown, which limits the functionality of the equipment and does not contribute to solving the problem of reducing the energy intensity of the process.

Considering the above, the task of predicting the impact of the shear action of the grinding load on the energy intensity

and productivity of fine grinding by abrasion in a tumbling mill appears to be quite relevant.

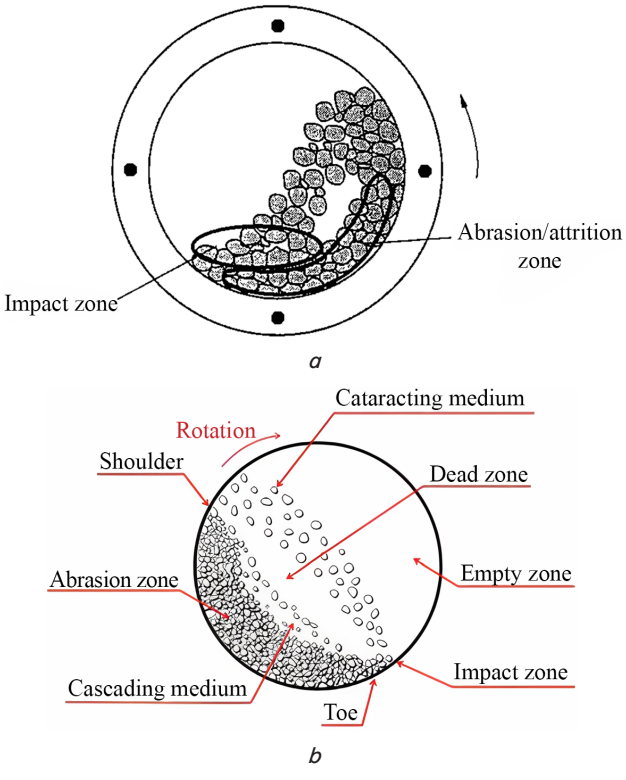

Fig. 1. Schematic representation of the occurrence of an abrasion zone in the intra-chamber loading of a tumbling mill: *a* — according to [5]; *b* — according to [9]

2. Literature review and problem statement

The implementation of grinding mechanisms in a tumbling mill is determined by the mode of movement of the intra-chamber loading, the modeling of which is associated with significant difficulties. Grinding by abrasion takes place in the zone of the shear layer of the rotating chamber load, where the mode of fast gravity flow occurs [10]. A feature of such a flow is the rapid displacement of particles of the granular medium, as a result of which they acquire a significant speed of chaotic movement and active interaction, which was not taken into account in [10]. Instead, the degree of activity of the mutual movement of particles of the intra-chamber load determines the intensity of the flow of the process of fine grinding in it. To intensify this process, it is necessary to activate the interaction in the shear layer.

Video recording of the behavior of the shear layer of the ball milling loading of the tumbling mill under the cascade mode of movement is given in [11]. However, quantitative characteristics of the shear interaction in this zone were not established in [11].

In works [12, 13], the geometric parameters of the loading shear layer zone were studied using X-ray spectroscopy. The structuring of the elements of the zone and their geometric characteristics were clarified and differentiated. The position of the free surface of the shear layer was established in [12]. The loading circulation center was found in [13]. However, the analysis of the dynamic parameters of movement in the shear layer was not carried out.

Shear flows of granular media remain the subject of intensive research. Special attention is paid to gravity-initiated shear flows due to their wide application value for numerous technological objects.

In addition, the abiding scientific interest in the study of flows in granular media is sustained spontaneously because of the rich phenomenology exhibited by granular materials. Depending on the scale of the process and the conditions of its existence, granular materials can exhibit the properties of a deformed solid, liquid, or gas [14]. This is accompanied by a growing number of fundamental problems associated with the need to explain such properties [15]. Various phenomenology of granular materials can be observed on the example of quartz sand, which can serve as a solid foundation for huge building structures and flow like a liquid in an hourglass or a gas during the expansion of dunes [16]. However, predicting the behavior of granular media remains quite problematic.

Among the many problems of fundamental importance, issues related to the formulation of defining ratios describing various rheological behavior of non-cohesive granular materials stand out. Due to the problems of describing flows for this kind of materials, there are no relations similar to the Navier-Stokes equation for classical fluids. The problems of formulating universal relations for flows of granular materials are explained by their extraordinary physical properties, which testify to their mesoscopic discrete and heterogeneous physical nature. Among this kind of properties, the high and difficult to identify dissipative effects of particle interaction and the difficulty of identifying the principles of transition from the characteristics of the object at the micro level (at the level of an individual particle) to the macroscopic characteristics of the flow are decisive. The broad unpredictable phenomenology of flows in granular media is still elusive. And there is no strict theoretical basis that can open in the near future access to the description of various forms of behavior of observed granular environments.

As a result, depending on the rate of shear deformation, three characteristic manifestations of the behavior of granular materials can be roughly distinguished: solid, liquid, and gaseous [14–16]. When describing these manifestations, the movement of materials is conditionally divided into two idealized regimes.

Under the first regime of slow or plastic flow, the particles of the medium move along some specific trajectories, being in continuous sliding contact with each other. Internal stresses in the environment arise as a result of dry Coulomb friction acting between them. This leads to a quasi-solid plastic behavior independent of the rate of deformation within the framework of the theory of limit equilibrium [17].

The quasi-liquid and gaseous behavior of granular materials is described by the second idealized mode of rapid motion [18]. Particles of a granular medium move chaotically, similar to molecules in a dense gas or liquid. Internal stresses in the medium arise as a result of momentum transfer, similar to how it occurs in a liquid or gas. Such a mechanism of the emergence of stresses leads to a significant dependence of them on the speed of displacement.

At moderate rates of deformation, the regime of shear flow of a granular liquid is realized [19, 20], in which the granular material exhibits viscoplastic properties. Under this mode, stresses are generated as a result of frictional and impact interactions of particles. This mode is characteristic of self-gravitational gravity currents, including in the chamber of a rotating drum.

At high deformation rates, a regime of rapid flow of granular gas is observed. This mode is accompanied by rapid impact contact interactions. An exemplary manifestation of such a flow is a boiling layer of granular material blown through a perforated support surface.

The physical parameter characterizing the energy of mutual movement of granular particles is the granular temperature [19]. This characteristic of the flow of a liquefied granular medium has been known for a long time and has undergone extensive applied testing [20]. It proved the high efficiency of application for numerical and experimental modeling [21]. It is believed that the concept of granular temperature, as a measure of velocity fluctuations in a fluidized granular system, was first put forward by Ogawa in 1978 [22, 23]. However, the temperature parameter was not involved to evaluate the shear interaction of the intra-chamber loading of the rotating drum.

Despite the lack of a direct method for measuring granular temperature, its effects are measurable and quite important. The temperature of a granular system can be found either by detailed measurement of particle velocities in numerical simulations, or experimentally, or indirectly through its consequences.

Extensive development and expansion of the concept of granular temperature during the last decade is associated with its application to the modeling of shearing gravity granular flows. The concept of granular temperature was extended to describe the behavior of dense granular systems to quantify the configuration of disordered force chains of particles [24]. In [25], dual granular temperatures are considered to account for two types of fluctuations of granular particles. At the same time, the creation of the theory of double granular temperatures is considered as an extension of the granular hydrodynamics of the granular medium. The configurational granular temperature was introduced to describe elastic energy fluctuations due to the evolution of the internal structures of the granular medium [26]. This temperature is considered an analog of the classical kinetic granular temperature, which is attributed to the translational degrees of freedom of granular particles.

The specified expansion of the concept made it possible to develop effective applied methods for determining the granular temperature of the granular flow in the chamber of a rotating drum. Speckle-Visible Spectroscopy (SVS) was used to measure the granular temperature of an avalanche-like collapse of a granular loading chamber of a slowly rotating drum at half degree of filling. It is shown that the temperature increases with an increase in the speed of rotation [27]. In [28], the SVS method was used to measure the granular temperature of the passive layer of an avalanche-like collapse of a chamber loading. It is shown that the temperature distribution of granules in the passive layer is not symmetrical. It turned out that the temperature of non-spherical particles rises sharply before the collapse, then sharply decreases to zero after the avalanche, in contrast to the behavior of spherical particles [29]. In [30], steady and non-steady states of an avalanche occurring alternately were established. In the stationary state, the granular temperature is low, and in the non-stationary state, it is significant, because intense relative movements occur between the grains in the active layer. Taking advantage of the high temporal and spatial resolution of SVS, the granular temperature distribution in such a passive loading layer was measured [31]. In [32], granular temperature was measured by SVS and discrete element (DEM) methods. The temperature of the active layer was approximately 5–8 times higher than the temperature of the passive layer. However, the influence of temperature on the grinding process by abrasion was not considered.

The granular temperature is a thermodynamic analogy with the thermal motion of molecules, which characterizes the specific kinetic energy of oscillations of granular particles in a shear flow. Factors of the granular temperature can be fluctuations, shifts, and transverse mutual movement of particles [33]. However, the conceptual approaches to the formalization of the granular temperature formulated in known works do not make it possible to numerically establish the parameters of the shear interaction of the particles of the intra-chamber loading of the tumbling mill.

Individual characteristics of the manifestation of the granular temperature of movement of the granular loading of the chamber of the rotating drum were studied by numerical methods. Using the molecular dynamics algorithm in [34], a pattern of the distribution of the granular temperature in the shear layer of monogranular loading was obtained for one speed of rotation of the chamber. In [35], a three-dimensional mathematical model based on the Euler approach and the kinetic theory of granular flow was used. It was established that the granular temperature acquires significant values only in the shear layer of loading. Using the DEM finite element method in [36], an increase in the temperature value in the lower part of the shear layer transitioning into the solid zone was detected. In [37], when applying the DEM method, it was shown that the granular temperature of granular particles of non-spherical shape acquires a maximum value on the surface of the shear layer. However, the obtained numerical results are only of a qualitative nature and do not allow for a quantitative assessment of the temperature manifestation in the shear layer.

Granular temperature parameters were studied experimentally by the method of visualization of loading movement through the transparent end wall of the chamber. In work [38], the behavior of a granular load that half-fills a slowly rotating chamber with a diameter of 0.39 m was studied using photo-fixation of movement patterns. A temperature profile was obtained, which proved its growth along the slope and in the direction of the free surface of the shear layer. However, the results reported in [38] have a non-systematic selective character.

In a number of works, video recording of loading movement was used to measure the granular temperature by particle velocity fluctuations. In [39] it was established that the temperature has a maximum value on the free surface of the layer. The influence of the humidity of the granular loading and the speed of rotation of the chamber on the granular temperature was studied in [40]. A decrease in temperature with an increase in humidity and an increase in temperature with an increase in rotation speed were revealed. In [41], a sharp decrease in temperature along the height of the shear layer in the direction from the free surface was established. However, the results do not allow us to quantitatively estimate the energy of the shear loading interaction.

In works [42–45], a video motion analyzer was used to record the granular temperature of loading in the form of a granular mixture. In [42], it was found that the temperature of a mixture of granular material with a liquid decreases with an increase in the viscosity of the liquid. The change in the granular temperature of a mixture of two granular materials with different densities was studied in [43]. It was established that the temperature decreases with an increase in the speed of rotation and the degree of filling of the chamber with the load. It is shown that an increase in the temperature

gradient causes an increase in the segregation of the granular mixture. The parameters of the granular temperature of a mixture of granular particles with finely dispersed material were considered in [44]. An increase in the loading temperature with an increase in the content of the fine fraction was revealed. In [45], the effect of a small amount of fine fraction on the loading temperature was studied. It has been shown that the addition of even a small amount of this fraction significantly increases the temperature. However, the results are mostly qualitative in nature and have not been generalized.

In a number of works, the experimental method of fluoroscopy of the movement of SVS granular particles was used to study the kinetic parameters of loading. In [46], SVS was used to determine the velocity distribution in the shear layer at steady motion of loading, but the granular temperature was not determined. An overview of works on the application of speckle spectroscopy to measure the granular temperature of loading a rotating drum is given in [33]. A conclusion on the effectiveness and perspective of this method of experimental research is drawn. However, no generalized numerical results regarding the interaction in the shear loading layer were obtained. In [27], the SVS method was applied to determine the granular temperature of the collapse of a granular avalanche on the free surface of the shear layer of the loading of a slowly rotating drum. A linear increase in the average value of the maximum temperature with increasing rotation speed was revealed. However, the obtained results apply only to unstable transient loading motion modes. With the help of SVS, the phenomenon of increased segregation of the granular mixture with an increase in the granular temperature gradient was established in [47]. However, the obtained data do not allow one to estimate the shear interaction energy. In [32], a comparative analysis of the effectiveness of determining the granular temperature of loading a rotating drum using the SVS experimental method and the DEM analytical method was performed. A good convergence of the results of the application of these methods is shown. However, the obtained sample results were not generalized.

Modeling of the movement zones of the granular loading chamber of the rotating drum was performed using the analytical-experimental method. The calculation algorithm was developed in [48]. In [49], patterns of motion were determined based on the position of the boundary between the solid-state zone and the flight zone. The characteristics of the shear layer were obtained in [50]. However, the results did not provide for the evaluation of the parameters of the abrasive grinding process.

In works [51–55], the characteristics of the active zones of loading movement were studied by the visualization method. In [51], parameters of self-oscillating loading action and grinding characteristics for discrete filling of the chamber were estimated.

The influence of the degree of filling on self-oscillating grinding for a discrete content of crushed material in the load is considered in [52]. In [53], the influence of the material content on loading motion modes and self-oscillating grinding for discrete chamber filling was investigated. The influence of the simultaneous change of filling and material content on grinding was studied in [54]. In [55], the mechanism of the loss of flow stability of the grain loading chamber of a rotating drum was revealed. Qualitative conditions for stability of motion of a dynamic system of a tumbling mill are established in [56]. However, the results correspond only to the self-oscillatory regime of the loading flow.

Mathematical models for two grinding mechanisms in a tumbling mill were built on the basis of data visualization. In work [11], the mechanism of destruction by breaking under the action of the impact loading mechanism was established. In [10], the mechanism of crushing failure under the action of the compression loading mechanism was revealed. The influence on the performance of the mass fractions of the movement zones, loading turnover and rotation speed was taken into account. However, the results refer only to performance in impact and compression grinding.

Our review of the literature [1–56] has made it possible to draw a conclusion regarding the content of the unsolved problem. It consists in the lack of models for determining the performance of the abrasive action of the grinding load on the material crushed in a tumbling mill. This is caused by the difficulties of analytical and numerical modeling and the complexity of the instrumental experimental study of the behavior of the shear layer of the granular loading chamber of the rotating drum. The impossibility of practical application of such models is especially negatively manifested in the case of the implementation of the energy-saving process of fine and ultrafine grinding.

3. The aim and objectives of the study

The purpose of our work is to build a mathematical model of the loading mechanism by the shear action of the grinding bodies of intra-chamber loading on the particles of the material crushed in the tumbling mill. This will make it possible to establish the dynamic characteristics of the shear action of grinding loading and predict the parameters of the grinding process by implementing the mechanism of destruction by abrasion.

To achieve this goal, the following tasks were solved:

– to perform analytical modeling and set the parameters of the shear interaction of the intra-chamber loading of the tumbling mill;

– to perform experimental modeling and evaluate the effect of rotation speed on the energy and productivity of the abrasion grinding process due to the implementation of the shear interaction mechanism.

4. The study materials and methods

4. 1. The object and hypothesis of the study

The object of our study is the shear grinding process in a tumbling mill. The subject of the study is the mathematical modeling of the process of shear loading, which causes the realization of the mechanism of destruction by abrasion.

It was assumed that the shear interaction of loading elements is carried out in the shear layer. The influence of shock and compressive interaction forces on the grinding process was neglected.

The basis of the model of the abrasion grinding mechanism was based on the relative dynamic parameters of the shear interaction, which are criteria for the similarity of the loading movement and the grinding process. The power of the shear interaction was considered to be an analog of the productivity of the abrasion grinding process.

The interaction of the chamber with the load was assumed mainly on a cylindrical surface. The influence of the end walls of the chamber on the movement of loading was neglected.

It was assumed that the mode of movement of the load in the chamber of the rotating drum is stable. The factors of the parameters of this regime were considered to be the stationary patterns of loading movement.

A simplified case of monofractional loading of a chamber of a rotating drum was considered. A discrete value of 0.45 was taken as the degree of filling of the chamber, which corresponds to the grinding process in a tumbling mill with a high throughput at the output of the finished product.

4. 2. Research methods

Since the boundary marginal effect of the loading flow on the end wall of the chamber turned out to be insignificant, the physical visualization of the data was adopted as a method of experimental research.

An experimental numerical modeling method based on experimental visualization of loading behavior in a rotating drum chamber was applied to determine shear interaction parameters. Visualization was carried out by registration through a transparent end wall and further processing of pictures of loading movement in the cross-section of the chamber. The algorithm for implementing the data visualization method consists in the sequential implementation of a number of stages [10, 11]. The calculation scheme of the pattern of the three-phase mode of movement of loading in the cross section of the rotating chamber is applied (Fig. 2). According to the scheme, the shear interaction is determined by the method of numerical modeling. The visualized geometric parameters are highlighted in color:

1) the radial coordinate of the base of the central averaged normal section of the shear layer R_{sl0};

2) the height of the central averaged normal cross section of the shear layer h_{sl};

3) the angle of inclination of the base of the central averaged normal cross section of the shear layer to the horizontal α_{sl};

4) the area of the shear layer zone F_{sl} (F_{BEGDB});

5) the radial coordinate of the loading circulation center R_c;

6) the radius of the cylindrical surface of the chamber R.

The values of these geometric parameters were used as input data for model calculations.

The vertical distance from the highest to the lowest point on the free surface of the flight zone h_{fr} was adopted in [11] as a visual input parameter that approximately determines the impact interaction (Fig. 2). R_{sl0} and h_{sl} (Fig. 2) were considered visual input characteristics of compressive interaction in [10]. At the same time, the mass fractions of the movement zones were visually determined by the ratio of the areas of the solid zone F_{sr} and F_{sl}, taking into account the dilatancy of the shear layer zone υ_{sl}. Load turnover was visually estimated by R_c.

Distinctive features of the application of the method for studying the shear interaction of loading are the use of the angle of inclination of the base of the cross-section as an additional visual input parameter and the use of a specialized calculation algorithm (Fig. 2). The simulation cycle in the part of experimental visualization of data for one speed of rotation of the drum consisted in the implementation of the following stages:

1) obtaining a pattern of the loading movement for the current value of the drum rotation speed;

2) visualization of the BEGDB shear layer zone by selection on the pattern;

3) visualization of the central averaged normal section of the shear layer by selection on the resulting pattern;

4) visualization of data R_{sl0}, h_{sl}, α_{sl}, F_{sl} (F_{BEGDB}), R_c, R by measuring on the pattern;

5) visualization of data υ_{sl} by evaluating the pattern;

6) calculation of the values of parameters of the shear interaction of the loading according to the corresponding expressions;

7) obtaining a pattern of loading movement for the next value of the drum rotation speed and transition to a new simulation cycle.

A stroboscopic tachometer was used to measure the rotational speed. The error of velocity measurements was approximately ±3 % when using error propagation analysis. Five times the steady-state rotational speed measurement for one loading motion mode was performed to estimate the error.

Measurements of linear dimensions and areas of geometric figures on motion patterns were carried out using available specialized computer applications of Kompas 3D, AutoCAD, and SolidWorks systems.

The size of the loading particles was measured by a laser-type analyzer.

Dosing of the loading portion was carried out using laboratory beakers. Portion volume was measured at rest.

3 motion patterns were obtained for one value of the rotation speed ψ_ω to exclude the influence of random factors on the reliability of the measurement results. For each speed of rotation, the deviations of the results of measurements of linear dimensions and areas of geometric figures in motion patterns were 2–3 %.

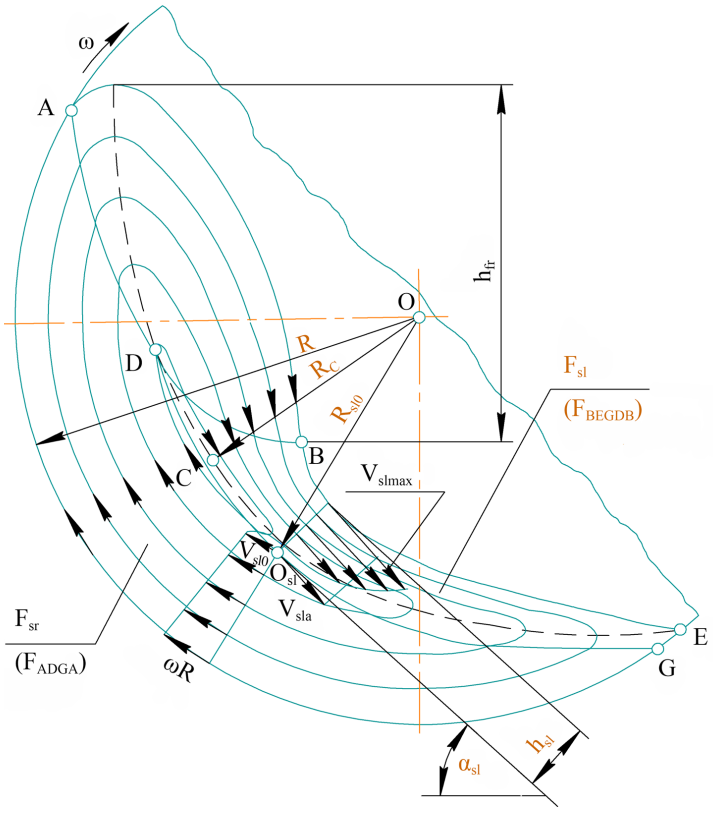

Fig. 2. Calculation diagram of the movement pattern with flow lines of granular loading in a chamber of radius R of a drum rotating with an angular velocity ω

Graphical and statistical procedures for processing the results of the experiments corresponded to the set tasks.

The errors of the obtained measurement results were determined and estimated, the values of which depended on the speed of rotation during experimental research.

The degree of filling $\kappa=w/(\pi R^2 L)$ estimated the contents of the loading chamber, where w is the volume of the loading portion at rest, R is the radius of the chamber, and L is the length of the chamber. The degree of filling was a discrete value of $\kappa=0.45$.

The relative velocity $\psi_\omega=\omega\sqrt{R/g}$ estimated the rotation speed of the drum, where ω is the angular velocity, g is the gravitational acceleration. The speed of rotation varied in the range from the state of rest to the limit of the transition of the circulation mode of loading motion to the wall layer mode. The step of changing the discrete value of the relative speed of stationary rotation was $\Delta\psi_\omega=0.05$.

Loose granular material with spherical particles with mean absolute d and relative size $\psi_d=d/(2R)=0.0104$ was used as loading. The value of the angle of internal friction of the material was 30°.

5. Research results regarding the grinding process in a tumbling mill with an abrasive action

5. 1. Results of analytical modeling of shear interaction of intra-chamber loading of a tumbling mill

The initial characteristic that approximately determines the amount of shear interaction is the average value of the shear velocity gradient in the central averaged normal section of the shear layer G_{sl}:

$$G_{sl}=\frac{V_{sl\max}+V_{sl0}}{h_{sl}}, \tag{1}$$

where

$$V_{sl\max}=\sqrt{2W_i\sin\alpha_{sl}\frac{\cos\varphi}{1-\sin\varphi}h_{sl}-V_{sl0}^2}$$

is the maximum shear rate in the central averaged normal section of the shear layer [50]; $V_{sl0}=\omega R_{sl0}$ – shear velocity of the support surface of the central averaged normal section of the shear layer; h_{sl} is the height of the central averaged normal section of the shear layer; R_{sl0} is the radial coordinate of the base of the central averaged normal section of the shear layer; α_{sl} is the angle of inclination of the base of the averaged normal section of the shear layer to the horizontal; φ is the angle of internal friction of granular loading;

$$W_i=g+a_{fr}=\sqrt[3]{-\frac{L}{2}+\sqrt{f}}+\sqrt[3]{-\frac{L}{2}-\sqrt{f}}-\frac{q}{3}$$

– imaginary total vertical acceleration of the shear layer, which causes its movement; a_{fr} is the imaginary additional inertial acceleration of the shear layer due to the increase in kinetic energy after the impact interaction of the flight zone with the shear layer [49]; f, L, q, m, c, d are component expressions selected to simplify the final expression for W_i:

$$f=\left(-\frac{q^2}{9}+\frac{m}{3}\right)^3+\left(\frac{L}{2}\right)^2,$$

$$L=2\left(\frac{q}{3}\right)^3-\frac{qm}{3}-2\frac{V_{sl0}^6}{d^3},$$

$$q=-\frac{1}{d^3}\left(\frac{V_{sla}^2}{c^2}+3d^2V_{sl0}^2\right),$$

$$m=\frac{1}{d^3}\left(2\frac{V_{sla}}{c}V_{sl0}^3+3dV_{slo}^4\right),$$

$$c=\frac{1-\sin\varphi}{3h_{sl}\sin\alpha_{sl}\cos\varphi},$$

$$d=\frac{2h_{sl}\sin\alpha_{sl}\cos\varphi}{1-\sin\varphi},$$

$$V_{sla}=\frac{\omega\left(R^2-R_{sl0}^2\right)}{2h_{sl}}$$

– the average value of the movement speed in the central averaged normal section of the shear layer.

The relative shear velocity gradient in the central averaged normal section of the shear layer G_{slr} corresponds to the ratio of the absolute gradient to the value of the critical angular velocity of rotation of the cylindrical surface of the drum chamber $\sqrt{g/R}$:

$$G_{slr}=G_{sl}\sqrt{\frac{R}{g}}. \tag{2}$$

After the transformations, expression (2) takes the form:

$$G_{slr}=\frac{V_{sl\max}+V_{sl0}}{h_{sl}}\sqrt{\frac{R}{g}}. \tag{3}$$

The amount of work of the forces of shear interaction is determined from their correspondence to the change in the kinetic energy of the impulse interaction during the mutual chaotic movement of particles in the shear loading layer.

The analog of the specific relative work of shear interaction forces corresponds to the averaged value of the granular temperature T_{sl} in the central averaged normal section of the shear loading layer:

$$T_{sl}=G_{slr}^2. \tag{4}$$

After the transformations, expression (4) takes the form:

$$T_{sl}=\frac{\left(V_{sl\max}+V_{sl0}\right)^2R}{h_{sl}^2g}. \tag{5}$$

The relative energy of abrasion grinding in one circulation cycle of loading in the chamber of a rotating drum E_{abrc} corresponds to the total relative work of the forces of shear interaction in one circulation cycle:

$$E_{abrc}=T_{sl}K_{sl}, \tag{6}$$

where K_{sl} is the mass fraction of the loading shear layer zone.

The expression for K_{sl} takes the form [10]:

$$K_{sl}=\frac{m_{sl}}{m}, \tag{7}$$

where m_{sl} is the mass of the loading shear layer; m is the mass of the entire load.

The value of K_{sl} can be approximately determined by the method of visualizing loading movement patterns by the expression:

$$K_{sl} = \frac{F_{sl}}{\pi R^2 \kappa \upsilon_{sl}}, \quad (8)$$

where F_{sl} is the area of the shear layer zone in the movement pattern; υ_{sl} is the dilatancy of the shear layer.

Since the increase in the volume of the shear layer during movement is small, the value of its dilatancy tends to zero $\upsilon_{sl} \to 1$.

After transformations, expression (6) takes the form:

$$E_{abrc} = \frac{\left(V_{slmax} + V_{sl0}\right)^2 R}{h_{sl}^2 g} K_{sl}. \quad (9)$$

The relative energy of grinding by abrasion in one revolution of the drum E_{abrt} corresponds to the complete relative work of the forces of shear interaction in one revolution:

$$E_{abrt} = E_{abrc} n_{to}, \quad (10)$$

where n_{to} is the turnover of the load movement, which determines the number of cycles of the load circulation in the chamber during one revolution of the drum.

The expression for n_{to} takes the form [11]:

$$n_{to} = \frac{2\pi}{t_{cp}\omega}, \quad (11)$$

where t_{cp} is the duration of the load circulation period in the rotating drum chamber.

The value of n_{to} can be roughly determined by the method of visualizing loading movement patterns by the expression:

$$n_{to} = \left[1 - \left(\frac{R_c}{R}\right)^2\right] \frac{1}{\kappa}, \quad (12)$$

where R_c is the radial coordinate of the load circulation center relative to the axis of rotation in the movement pattern.

After transformations, expression (10) takes the form:

$$E_{abrt} = \frac{\left(V_{slmax} + V_{sl0}\right)^2 R}{h_{sl}^2 g} K_{sl} n_{to}. \quad (13)$$

An analog of the relative productivity of abrasion grinding Q_{abr} corresponds to the relative strength of the forces of shear interaction:

$$Q_{abr} = \frac{E_{abrt}}{T_{tr}}, \quad (14)$$

where $T_{tr} = T_t \sqrt{g/R}$ is the relative period of rotation of the drum [10]; $T_t = 2\pi/\omega$ is the absolute period of rotation.

After transformations, expression (14) takes the form:

$$Q_{abr} = \frac{\left(V_{slmax} + V_{sl0}\right)^2 R}{2\pi h_{sl}^2 g} K_{sl} n_{to} \psi_\omega. \quad (15)$$

The applied relative parameters (2) to (15) are dynamic criteria for the similarity of loading movement and grinding process in a tumbling mill by abrasive action. The values of the dynamic parameters according to expressions (3), (5), (9), (13), and (15) make it possible to numerically evaluate the changes in the technological effect of the abrasive action of loading depending on the initial characteristics of the grinding process.

5. 2. Results of experimental modeling of shear interaction of intra-chamber loading of a tumbling mill

On the basis of data visualization, patterns of loading movement in the rotating drum chamber at κ=0.45 were obtained [11]. Separate obtained patterns of steady movement of loading in the chamber of a stationary rotating drum are shown in Fig. 3. Patterns were acquired for the range of values of the relative speed of rotation ψ_ω=0.05–1.3 with a step of $\Delta\psi_\omega$=0.05. The obtained patterns characterize the influence of the speed of rotation on the geometric characteristics of the load movement zones in the drum chamber.

The simulation cycle in the part of calculating the parameters of the shear interaction of the load based on the received visual data of the geometric characteristics for one speed of rotation of the drum included the following stages:

1) obtaining a pattern of the loading movement for the rotation speed ψ_ω;

2) visualization of input data R_{sl0}, h_{sl}, α_{sl}, F_{sl}, R_c, R by measurement on the pattern and visualization of υ_{sl} by evaluation on the pattern;

3) calculation of the relative shear velocity gradient in the section of the G_{slr} loading shear layer according to (3) based on the visualized data R_{sl0}, h_{sl}, α_{sl}, R;

4) calculation of the granular temperature in the section of the shear layer loading T_{sl} according to (5) based on the visualized data R_{sl0}, h_{sl}, α_{sl}, R;

5) calculation of the mass fraction of the zone of the shear layer loading K_{sl} according to (8) based on the visualized data F_{sl}, R, υ_{sl};

6) calculation of the relative energy of grinding by abrasion for one cycle of loading circulation in the chamber of the rotating drum E_{abrc} according to (9) based on the visualized data R_{sl0}, h_{sl}, α_{sl}, F_{sl}, R, υ_{sl};

7) calculating the turnover of loading movement n_{to} according to (12) based on visualized data R_c, R;

8) calculation of the relative grinding energy by abrasion for one rotation of the drum E_{abrt} according to (13) based on the visualized data R_{sl0}, h_{sl}, α_{sl}, F_{sl}, R_c, R, υ_{sl};

9) calculation of the analog of the relative productivity of abrasion grinding Q_{abr} according to (15) based on the visualized data R_{sl0}, h_{sl}, α_{sl}, F_{sl}, R_c, R, υ_{sl};

10) obtaining a pattern of loading movement for the next value of rotation speed $\psi_\omega + \Delta\psi_\omega$ and transition to a new simulation cycle.

When visualizing the input data, the dependence of change in their values on the growth of the relative speed of rotation ψ_ω from the minimum value of 0.05 to the maximum value of 1.3 was evaluated. The ratio of the radial coordinate of the base of the central averaged normal section of the shear layer to the radius of the cylindrical surface of the chamber R_{sl0}/R varied from 0.19 to 1. The ratio of the central averaged normal section of the shear layer to the chamber radius h_{sl}/R varied from 0.091 at ψ_ω=0.05, reaching a maximum value of 0.26 at ψ_ω=0.55 and decreased to 0 at ψ_ω=1.3. The value of the inclination angle α_{sl} varied from 31° at ψ_ω=0.05, reached a maximum value of 55° at ψ_ω=0.5, and decreased to 0 at ψ_ω=1.3. The ratio of the area of the shear layer zone to the cross-sectional area of loading $F_{sl}/(\pi R^2 \kappa \upsilon_{sl})$ varied from 0 at ψ_ω=0.05, reached a maximum value of 0.2 at ψ_ω=0.4–0.45, and decreased to 0 at ψ_ω=1.3. The ratio of the radial coordinate of the loading circulation center to the chamber radius R_c/R varied from 0.083 to 0.74.

a *b* *c* *d* *e*

Fig. 3. Patterns of movement of granular loading with relative particle size ψ_d=0.0104 and degree of chamber filling κ=0.45: *a* – ψ_ω=0.1; *b* – ψ_ω=0.3; *c* – ψ_ω=0.5; *d* – ψ_ω=0.7; *e* – ψ_ω=0.9 (according to [11])

The plots of results from the experimental determination of change in dimensionless parameters of the shear interaction of loading at κ=0.45 are shown in Fig. 4–10. The plots are constructed in dimensionless axes: corresponding vertical G_{slr}, T_{sl}, K_{sl}, E_{abrc}, n_{to}, E_{abrt}, Q_{abr} and common horizontal ψ_ω.

The plot of change in the relative gradient of the shear velocity in the cross-section of the loading shear layer G_{slr} as a function of the relative rotation speed ψ_ω is shown in Fig. 4. G_{slr} values were calculated according to expression (3).

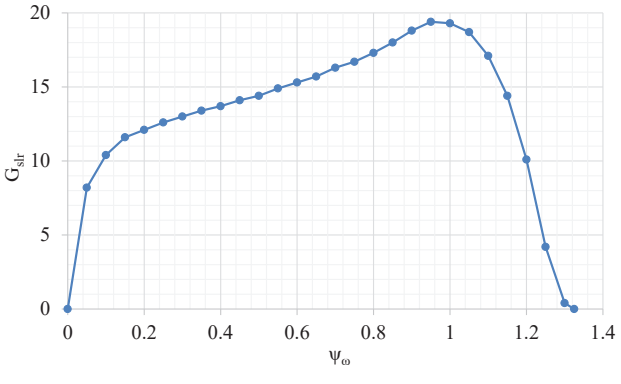

Fig. 4. Experimental dependence of change in the relative gradient of the shear velocity in the section of the shear layer G_{slr} on the relative speed of rotation ψ_ω

The plot of change in the granular temperature in the cross-section of the shear layer loading T_{sl} against the relative speed of rotation ψ_ω is shown in Fig. 5. T_{sl} values were calculated according to expression (5).

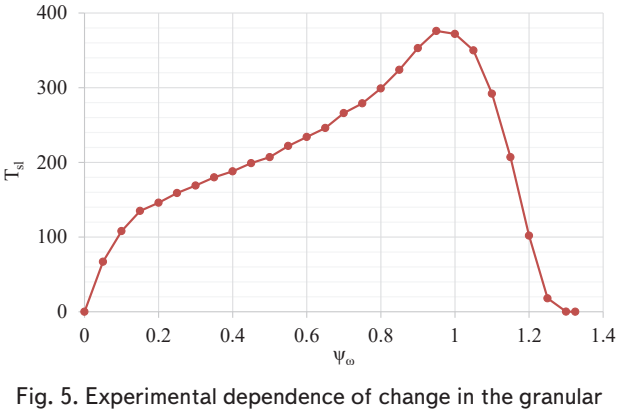

Fig. 5. Experimental dependence of change in the granular temperature in the cross-section of the shear layer T_{sl} on the relative speed of rotation ψ_ω

The plot of change in the mass fraction of the shear layer zone K_{sl} as a function of the relative speed of rotation ψ_ω is shown in Fig. 6 [10]. K_{sl} values were determined by expression (8).

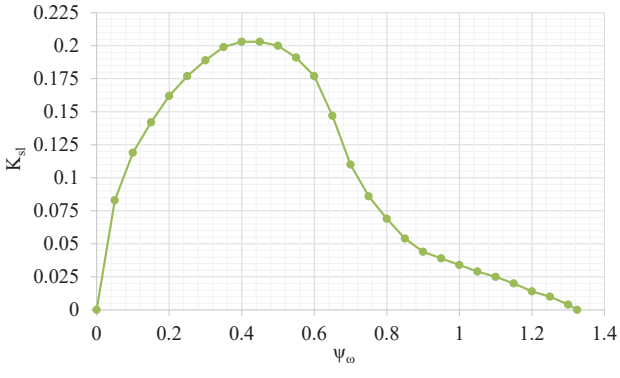

Fig. 6. Experimental dependence of change in the mass fraction of the shear layer zone K_{sl} on the relative speed of rotation ψ_ω (according to [10])

The plot of change in the relative energy of grinding by abrasion for one cycle of loading circulation in the chamber of the rotating drum E_{abrc} as a function of the relative speed of rotation ψ_ω is shown in Fig. 7. E_{abrc} values were calculated according to expression (9).

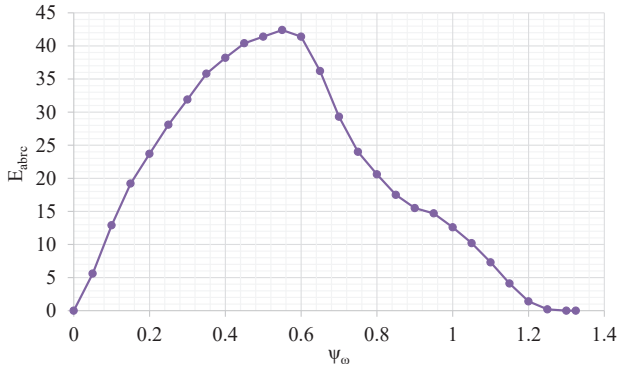

Fig. 7. Experimental dependence of change in the relative energy of grinding by abrasion during one cycle of loading circulation in the chamber of the rotating drum E_{abrc} on the relative speed of rotation ψ_ω

The plot of change in the turnover of the movement of loading n_{to} from ψ_ω is shown in Fig. 8. The values of n_{to} were determined by expression (12) [11].

The plot of change in the relative energy of grinding by abrasion in one revolution of the drum E_{abrt} versus the relative speed of rotation ψ_ω is shown in Fig. 9. E_{abrt} values were calculated according to expression (13).

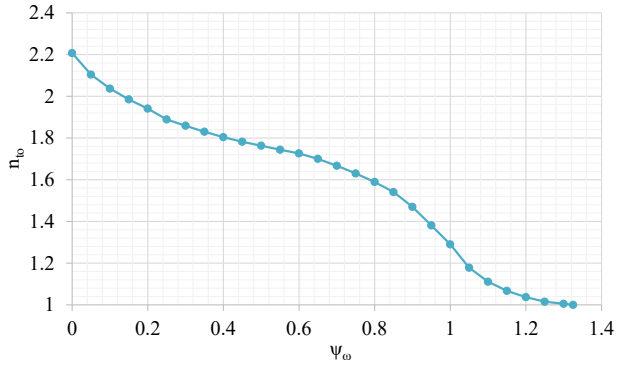

Fig. 8. Experimental dependence of change in the turnover of the loading movement n_{to} on the relative speed of rotation ψ_ω (according to [11])

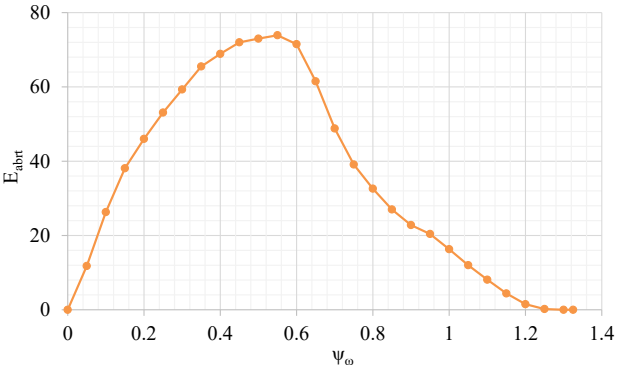

Fig. 9. Experimental dependence of change in the relative energy of grinding by abrasion in one revolution of the drum E_{abrt} on the relative speed of rotation ψ_ω

The plot of change in the analog of the relative productivity of abrasion grinding Q_{abr} from the relative speed of rotation ψ_ω is shown in Fig. 10. Q_{abr} values were calculated according to expression (15).

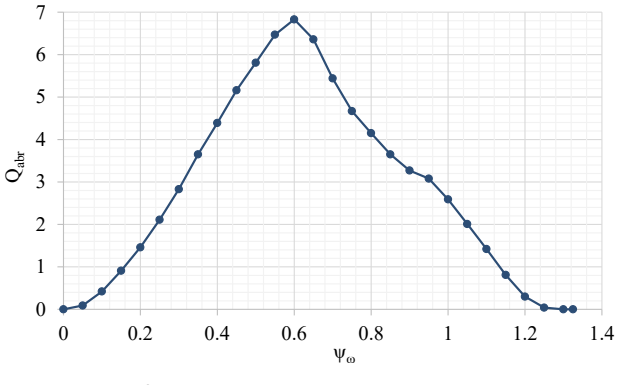

Fig. 10. Experimental dependence of change in the analog of the relative productivity of abrasion grinding Q_{abr} on the relative speed of rotation ψ_ω

The resulting experimental dependences of the numerical values of the parameters of the shear interaction of loading characterize the quantitative influence of the speed of rotation on the grinding process by abrasion in a tumbling mill.

6. Discussion of results of investigating the grinding process in a tumbling mill with an abrasive action

Our analytical and experimental modeling results have made it possible to evaluate the qualitative and quantitative influence of the loading motion characteristics of the rotating chamber on its shear interaction.

The visualized geometric parameters of patterns of movement of granular loading in the cross-section of the chamber of the rotating drum were used as the initial data of the model calculations in the criterion form.

The initial characteristic, which approximately determines the magnitude of the shear action, was revealed. This is the average value of the shear rate gradient in the central averaged normal section of the shear layer G_{sl} (1). The abrasive action is realized as a result of impulse interaction during the mutual chaotic movement of particles in the shear layer of loading and is characterized by the granular temperature T_{sl} (4).

It was established that the value of the analog of grinding performance in a tumbling mill by abrasion Q_{abr} (15) is proportional to the granular temperature T_{sl} (5). In addition, the performance is proportional to the value of the shear layer zone mass fraction K_{sl} [10], loading turnover n_{to} [11], and drum rotation speed ψ_ω. A significant effect on the performance of the mass fraction K_{sl}, which reaches its maximum value at the relative speed of rotation ψ_ω=0.4–0.45, was revealed [10]. The influence of n_{to} turnover increases with a decrease in ψ_ω [11]. The defining characteristic of the shear interaction is the speed of rotation, which determines the values of the parameters T_{sl}, K_{sl} and n_{to}.

The conditions for achieving the maximum values of the parameters of the shear interaction of loading have been established. The gradient of the shear rate G_{slr} (Fig. 4) and the granular temperature T_{sl} (Fig. 5) reach a maximum at the speed ψ_ω=0.95. Instead, the energy E_{abrc} (Fig. 7) and E_{abrt} (Fig. 9) reach a maximum at ψ_ω=0.55, and the productivity Q_{abr} (Fig. 10) – at ψ_ω=0.6. This is due to the fact that with a decrease in the speed of ψ_ω from 0.85 to 0.6–0.65, there is a significant, approximately 3-fold, increase in the mass fraction K_{sl} (Fig. 6). In addition, the turnover value n_{to} increases by 1.11 times (Fig. 8).

Analysis of Fig. 9, 10 proves that the rational range of rotation speed values for grinding in a tumbling mill by abrasion can be considered to be ψ_ω=0.5–0.6. At the same time, the values of energy E_{abrt} (Fig. 9) and productivity Q_{abr} (Fig. 10) of grinding by abrasion acquire a fraction of 0.85–0.97 and more, from the maximum possible values.

The comparative analysis proved the convergence with the known data of the individual results obtained regarding the determination of the shear interaction of the elements of the granular loading of the chamber of the rotating drum. The revealed relative values of the granular temperature T_{sl} (Fig. 5) of the shear loading layer complement and extend the similar results reported in [34, 36, 39] in terms of taking into account the influence of change in rotation speed.

The established recommendations for the rational range of rotation speed during abrasion grinding ψ_ω=0.5–0.6 coincide well with the data from [1, 57, 58] and GOST 10141-91 and its analogs [59, 60]. In these sources, the processes of medium grinding in tumbling mills were considered mainly by attrition during the shear interaction of loading. In [1, 57] it was experimentally shown that the energy intensity of dry

grinding of cement clinker, limestone, and quartz in a ball mill reaches a minimum at ψ_ω=0.55. In work [57], the speed of rotation ψ_ω=0.5–0.6 was experimentally established when reducing the energy intensity of the process of wet grinding of limestone. In [58], a speed of ψ_ω=0.6 was experimentally found for the highest productivity of wet grinding of iron ore in a laboratory ball mill. Standards GOST 10141-91 «Rod and ball mills. General technical requirements» and [59, 60] normalize the processes of wet grinding of ore and non-ore minerals in tumbling mills. According to these standards, the normative speed of rotation of core tumbling mills with peripheral unloading is ψ_ω=0.55–0.65.

The difference between the rational values of the rotation speed for grinding in a tumbling mill by abrasion under the shear interaction of loading from grinding by compression and impact was found. The comparative analysis concerned the results of work and papers [10, 11], which were obtained for the same modeling conditions. It turned out that the efficiency of grinding by abrasion is achieved at a lower speed of rotation ψ_ω=0.5–0.6. Instead, the rational speed for crushing by compression is ψ_ω=0.55–0.65, and by impact – ψ_ω=0.75–0.9.

Our results make it possible to solve the problem of approximate mathematical modeling based on data visualization of the grinding mechanism in the tumbling mill by abrasion when implementing the shear loading mechanism. The mathematical mode builtl makes it possible to carry out a comparative analysis of the effect of material destruction by abrasion, impact, and crushing on the grinding process. This will make it possible to predict the energy consumption of grinding when the defining characteristics of the process are changed – the speed of rotation and the degree of filling the chamber with the load. Since grinding by abrasion, impact, and crushing is related to the tonnage of grinding, the resulting model also enables the prediction of the particle size composition of the final product.

The field of application of our results is the implementation of the process of fine grinding at the last stage of grinding. The condition for using the results is a reasonable change in the parameters of the traditional working processes of tumbling mills. The potentially expected effect of use is to reduce the energy consumption of the grinding process by rationally changing the speed of rotation, the degree of filling of the chamber, and the content of the grinding material.

The applicability of the established dynamic characteristics of the shear interaction and the results of forecasting the parameters of the fine and ultrafine grinding process by implementing the abrasion mechanism is limited by the discrete values of the input parameters. The accepted value of the degree of filling of the drum chamber with loading was κ=0.45, corresponding to the grinding process in a tumbling mill with a high throughput. The size of the loading grinding bodies relative to the chamber diameter was 0.0104.

The use of one discrete value of the degree of filling can be interpreted as a drawback of this study, which imposes certain restrictions on the application of the results. It seems that a potentially interesting area of further research is the identification of the characteristics of interaction of elements with a different, in particular, a smaller filling of the chamber with loading. This will reveal new dynamic effects of the abrasion grinding mechanism.

In the future, it is expedient to experimentally find out the technological and energy efficiency of grinding with the joint action of impact, compression, and shear loading mechanisms on the particles of the crushed material. This will make it possible to establish rational conditions for the implementation of mechanisms for destruction by breaking, crushing, and abrasion during the implementation of energy-saving grinding processes in drum-type mills.

7. Conclusions

1. Analytical modeling of the abrasive action of the intra-chamber loading of a tumbling mill is based on the consideration of the displacement of granular particles. As a result, they acquire a significant speed of chaotic movement and active interaction. The shear interaction factor is the average value of the shear velocity gradient in the central averaged normal cross section of the shear layer. The abrasive action is realized as a result of impulse interaction during the mutual chaotic movement of particles in the shear layer of loading and is characterized by granular temperature. The analogs of the dynamic parameters of the shear interaction are the granular temperature, the work, and the power of forces of the impulse interaction of the particles. The relative strength of the forces of shear interaction can be taken as an analog of the relative performance of the abrasion grinding process. The applied relative dynamic parameters of the shear interaction are criteria for the similarity of the loading motion and the grinding process in the tumbling mill by attrition.

Determining parameters of the effect on the analog of grinding performance by abrasion are the velocity gradient and the mass fraction of the shear layer, the turnover of the loading circulation in the chamber and its rotation speed.

2. It was experimentally established that the energy of grinding by abrasion reaches its maximum value at the value of the relative speed of rotation of the drum chamber ψ_ω=0.55, and the analog of productivity is at ψ_ω=0.6. A rational condition for grinding in a tumbling mill by abrasion at a rotation speed of ψ_ω=0.5–0.6 was revealed. The established speed is lower, compared to the rational grinding conditions when crushing ψ_ω=0.55–0.65 and breaking ψ_ω=0.75.

Conflicts of interest

The authors declare that they have no conflicts of interest in relation to the current study, including financial, personal, authorship, or any other, that could affect the study and the results reported in this paper.

Funding

The study was conducted without financial support.

Data availability

All data are available in the main text of the manuscript.

Use of artificial intelligence

The authors confirm that they did not use artificial intelligence technologies when creating the current work.

References

1. Gupta, V. K. (2020). Energy absorption and specific breakage rate of particles under different operating conditions in dry ball milling. Powder Technology, 361, 827–835. https://doi.org/10.1016/j.powtec.2019.11.033
2. Góralczyk, M., Krot, P., Zimroz, R., Ogonowski, S. (2020). Increasing Energy Efficiency and Productivity of the Comminution Process in Tumbling Mills by Indirect Measurements of Internal Dynamics – An Overview. Energies, 13 (24), 6735. https://doi.org/10.3390/en13246735
3. Tavares, L. M. (2017). A Review of Advanced Ball Mill Modelling. KONA Powder and Particle Journal, 34, 106–124. https://doi.org/10.14356/kona.2017015
4. Semsari Parapari, P., Parian, M., Rosenkranz, J. (2020). Breakage process of mineral processing comminution machines – An approach to liberation. Advanced Powder Technology, 31 (9), 3669–3685. https://doi.org/10.1016/j.apt.2020.08.005
5. Napier-Munn, T. J., Morrell, S., Morrison, R. D., Kojovic, T. (1996). Mineral comminution circuits: their operation and optimisation. JKMRC Monograph series in mining and mineral processing, 2.
6. Ye, X., Gredelj, S., Skinner, W., Grano, S. R. (2010). Regrinding sulphide minerals — Breakage mechanisms in milling and their influence on surface properties and flotation behaviour. Powder Technology, 203 (2), 133–147. https://doi.org/10.1016/j.powtec.2010.05.002
7. Hasan, M., Palaniandy, S., Hilden, M., Powell, M. (2017). Calculating breakage parameters of a batch vertical stirred mill. Minerals Engineering, 111, 229–237. https://doi.org/10.1016/j.mineng.2017.06.024
8. Chen, X., Peng, Y., Bradshaw, D. (2014). The effect of particle breakage mechanisms during regrinding on the subsequent cleaner flotation. Minerals Engineering, 66-68, 157–164. https://doi.org/10.1016/j.mineng.2014.04.020
9. Wills, B. A., Finch, J. (2015). Wills' Mineral Processing Technology. Butterworth-Heinemann. https://doi.org/10.1016/c2010-0-65478-2
10. Naumenko, Y., Deineka, K. (2023). Building a model of the compression grinding mechanism in a tumbling mill based on data visualization. Eastern-European Journal of Enterprise Technologies, 5 (1 (125)), 64–72. https://doi.org/10.15587/1729-4061.2023.287565
11. Naumenko, Y., Deineka, K. (2023). Building a model of the impact grinding mechanism in a tumbling mill based on data visualization. Eastern-European Journal of Enterprise Technologies, 3 (7 (123)), 65–73. https://doi.org/10.15587/1729-4061.2023.283073
12. Morrison, A. J., Govender, I., Mainza, A. N., Parker, D. J. (2016). The shape and behaviour of a granular bed in a rotating drum using Eulerian flow fields obtained from PEPT. Chemical Engineering Science, 152, 186–198. https://doi.org/10.1016/j.ces.2016.06.022
13. de Klerk, D. N., Govender, I., Mainza, A. N. (2019). Geometric features of tumbling mill flows: A positron emission particle tracking investigation. Chemical Engineering Science, 206, 41–49. https://doi.org/10.1016/j.ces.2019.05.020
14. Jaeger, H. M., Nagel, S. R., Behringer, R. P. (1996). Granular solids, liquids, and gases. Reviews of Modern Physics, 68 (4), 1259–1273. https://doi.org/10.1103/revmodphys.68.1259
15. Forterre, Y., Pouliquen, O. (2008). Flows of Dense Granular Media. Annual Review of Fluid Mechanics, 40 (1), 1–24. https://doi.org/10.1146/annurev.fluid.40.111406.102142
16. Forterre, Y., Pouliquen, O. (2011). Granular Flows. Glasses and Grains, 77–109. https://doi.org/10.1007/978-3-0348-0084-6_4
17. Brown, R. L., Richards, J. C. (2016). Principles of powder mechanics: essays on the packing and flow of powders and bulk solids. Elsevier. https://doi.org/10.1016/c2013-0-01576-9
18. Savage, S. B. (1984). The Mechanics of Rapid Granular Flows. Advances in Applied Mechanics, 289–366. https://doi.org/10.1016/s0065-2156(08)70047-4
19. Campbell, C. (1990). Rapid Granular Flows. Annual Review of Fluid Mechanics, 22 (1), 57–92. https://doi.org/10.1146/annurev.fluid.22.1.57
20. Campbell, C. S. (2006). Granular material flows – An overview. Powder Technology, 162 (3), 208–229. https://doi.org/10.1016/j.powtec.2005.12.008
21. Jiang, Y., Liu, M. (2009). Granular solid hydrodynamics. Granular Matter, 11 (3), 139–156. https://doi.org/10.1007/s10035-009-0137-3
22. Ogawa, S. (1978). Multitemperature theory of granular materials. Proc. of the US-Japan Seminar on Continuum Mechanical and Statistical Approaches in the Mechanics of Granular Materials, 208–217.
23. Ogawa, S., Umemura, A., Oshima, N. (1980). On the equations of fully fluidized granular materials. Zeitschrift Für Angewandte Mathematik Und Physik ZAMP, 31 (4), 483–493. https://doi.org/10.1007/bf01590859
24. Sun, Q., Song, S., Jin, F., Jiang, Y. (2012). Entropy productions in granular materials. Theoretical and Applied Mechanics Letters, 2 (2), 021002. https://doi.org/10.1063/2.1202102
25. Sun, Q., Song, S., Liu, J., Fei, M., Jin, F. (2013). Granular materials: Bridging damaged solids and turbulent fluids. Theoretical and Applied Mechanics Letters, 3 (2), 021008. https://doi.org/10.1063/2.1302108
26. Sun, Q., Jin, F., Wang, G., Song, S., Zhang, G. (2015). On granular elasticity. Scientific Reports, 5 (1). https://doi.org/10.1038/srep09652
27. Yang, H., Li, R., Kong, P., Sun, Q. C., Biggs, M. J., Zivkovic, V. (2015). Avalanche dynamics of granular materials under the slumping regime in a rotating drum as revealed by speckle visibility spectroscopy. Physical Review E, 91 (4). https://doi.org/10.1103/physreve.91.042206

28. Li, R., Yang, H., Zheng, G., Zhang, B. F., Fei, M. L., Sun, Q. C. (2016). Double speckle-visibility spectroscopy for the dynamics of a passive layer in a rotating drum. Powder Technology, 295, 167–174. https://doi.org/10.1016/j.powtec.2016.03.031
29. Yang, H., Zhang, B. F., Li, R., Zheng, G., Zivkovic, V. (2017). Particle dynamics in avalanche flow of irregular sand particles in the slumping regime of a rotating drum. Powder Technology, 311, 439–448. https://doi.org/10.1016/j.powtec.2017.01.064
30. Li, R., Yang, H., Zheng, G., Sun, Q. C. (2018). Granular avalanches in slumping regime in a 2D rotating drum. Powder Technology, 326, 322–326. https://doi.org/10.1016/j.powtec.2017.12.032
31. Yang, H., Zhu, Y., Li, R., Sun, Q. (2020). Kinetic granular temperature and its measurement using speckle visibility spectroscopy. Particuology, 48, 160–169. https://doi.org/10.1016/j.partic.2018.07.011
32. Jing, Z., Yang, H., Wang, S., Chen, Q., Li, R. (2021). Comparison of granular temperature measured by SVS and DEM in the rotating cylinder. Powder Technology, 380, 282–287. https://doi.org/10.1016/j.powtec.2020.11.073
33. Dolgunin, V. N., Ivanov, O. O., Akopyan, S. A. (2020). Quasithermal Effects During Rapid Gravity Flow of a Granular Medium. Advanced Materials & Technologies, 3 (19), 047–055. https://doi.org/10.17277/amt.2020.03.pp.047-055
34. Li, S., Yao, Q., Chen, B., Zhang, X., Ding, Y. L. (2007). Molecular dynamics simulation and continuum modelling of granular surface flow in rotating drums. Chinese Science Bulletin, 52 (5), 692–700. https://doi.org/10.1007/s11434-007-0069-4
35. Yin, H., Zhang, M., Liu, H. (2014). Numerical simulation of three-dimensional unsteady granular flows in rotary kiln. Powder Technology, 253, 138–145. https://doi.org/10.1016/j.powtec.2013.10.044
36. Yang, S., Sun, Y., Zhang, L., Chew, J. W. (2017). Segregation dynamics of a binary-size mixture in a three-dimensional rotating drum. Chemical Engineering Science, 172, 652–666. https://doi.org/10.1016/j.ces.2017.07.019
37. Yang, S., Wang, H., Wei, Y., Hu, J., Chew, J. W. (2020). Flow dynamics of binary mixtures of non-spherical particles in the rolling-regime rotating drum. Powder Technology, 361, 930–942. https://doi.org/10.1016/j.powtec.2019.10.110
38. Longo, S., Lamberti, A. (2002). Grain shear flow in a rotating drum. Experiments in Fluids, 32 (3), 313–325. https://doi.org/10.1007/s003480100359
39. Chou, H.-T., Lee, C.-F. (2008). Cross-sectional and axial flow characteristics of dry granular material in rotating drums. Granular Matter, 11 (1), 13–32. https://doi.org/10.1007/s10035-008-0118-y
40. Chou, S. H., Hsiau, S. S. (2011). Experimental analysis of the dynamic properties of wet granular matter in a rotating drum. Powder Technology, 214 (3), 491–499. https://doi.org/10.1016/j.powtec.2011.09.010
41. Chou, S. H., Hu, H. J., Hsiau, S. S. (2016). Investigation of friction effect on granular dynamic behavior in a rotating drum. Advanced Powder Technology, 27 (5), 1912–1921. https://doi.org/10.1016/j.apt.2016.06.022
42. Liao, C.-C., Lan, H.-W., Hsiau, S.-S. (2016). Density-induced granular segregation in a slurry rotating drum. International Journal of Multiphase Flow, 84, 1–8. https://doi.org/10.1016/j.ijmultiphaseflow.2016.04.015
43. Liao, C.-C. (2019). Effect of dynamic properties on density-driven granular segregation in a rotating drum. Powder Technology, 345, 151–158. https://doi.org/10.1016/j.powtec.2018.12.093
44. Liao, C.-C., Ou, S.-F., Chen, S.-L., Chen, Y.-R. (2020). Influences of fine powder on dynamic properties and density segregation in a rotating drum. Advanced Powder Technology, 31 (4), 1702–1707. https://doi.org/10.1016/j.apt.2020.02.006
45. Chung, Y.-C., Liao, C.-C., Zhuang, Z.-H. (2021). Experimental investigations for the effect of fine powders on size-induced segregation in binary granular mixtures. Powder Technology, 387, 270–276. https://doi.org/10.1016/j.powtec.2021.04.034
46. Govender, I., Richter, M. C., Mainza, A. N., De Klerk, D. N. (2016). A positron emission particle tracking investigation of the scaling law governing free surface flows in tumbling mills. AIChE Journal, 63 (3), 903–913. https://doi.org/10.1002/aic.15453
47. Xiu, W., Li, R., Chen, Q., Sun, Q., Zivkovic, V., Yang, H. (2023). Prediction of segregation characterization based on granular velocity and concentration in rotating drum. Particuology, 73, 17–25. https://doi.org/10.1016/j.partic.2022.03.008
48. Naumenko, Y. (2017). Modeling a flow pattern of the granular fill in the cross section of a rotating chamber. Eastern-European Journal of Enterprise Technologies, 5 (1 (89)), 59–69. https://doi.org/10.15587/1729-4061.2017.110444
49. Naumenko, Y. (2017). Modeling of fracture surface of the quasi solid-body zone of motion of the granular fill in a rotating chamber. Eastern-European Journal of Enterprise Technologies, 2 (1 (86)), 50–57. https://doi.org/10.15587/1729-4061.2017.96447
50. Naumenko, Y., Sivko, V. (2017). The rotating chamber granular fill shear layer flow simulation. Eastern-European Journal of Enterprise Technologies, 4 (7 (88)), 57–64. https://doi.org/10.15587/1729-4061.2017.107242
51. Deineka, K., Naumenko, Y. (2019). Revealing the effect of decreased energy intensity of grinding in a tumbling mill during self-excitation of auto-oscillations of the intrachamber fill. Eastern-European Journal of Enterprise Technologies, 1 (1 (97)), 6–15. https://doi.org/10.15587/1729-4061.2019.155461
52. Deineka, K., Naumenko, Y. (2019). Establishing the effect of a decrease in power intensity of self-oscillating grinding in a tumbling mill with a reduction in an intrachamber fill. Eastern-European Journal of Enterprise Technologies, 6 (7 (102)), 43–52. https://doi.org/10.15587/1729-4061.2019.183291

53. Deineka, K., Naumenko, Y. (2020). Establishing the effect of decreased power intensity of self-oscillatory grinding in a tumbling mill when the crushed material content in the intra-chamber fill is reduced. Eastern-European Journal of Enterprise Technologies, 4 (1 (106)), 39–48. https://doi.org/10.15587/1729-4061.2020.209050
54. Deineka, K., Naumenko, Y. (2021). Establishing the effect of a simultaneous reduction in the filling load inside a chamber and in the content of the crushed material on the energy intensity of self-oscillatory grinding in a tumbling mill. Eastern-European Journal of Enterprise Technologies, 1 (1 (109)), 77–87. https://doi.org/10.15587/1729-4061.2021.224948
55. Deineka, K., Naumenko, Y. (2022). Revealing the mechanism of stability loss of a two-fraction granular flow in a rotating drum. Eastern-European Journal of Enterprise Technologies, 4 (1 (118)), 34–46. https://doi.org/10.15587/1729-4061.2022.263097
56. Deineka, K. Yu., Naumenko, Yu. V. (2018). The tumbling mill rotation stability. Scientific Bulletin of National Mining University, 1, 60–68. https://doi.org/10.29202/nvngu/2018-1/10
57. Gupta, V. K., Sharma, S. (2014). Analysis of ball mill grinding operation using mill power specific kinetic parameters. Advanced Powder Technology, 25 (2), 625–634. https://doi.org/10.1016/j.apt.2013.10.003
58. Hanumanthappa, H., Vardhan, H., Mandela, G. R., Kaza, M., Sah, R., Shanmugam, B. K. (2020). A comparative study on a newly designed ball mill and the conventional ball mill performance with respect to the particle size distribution and recirculating load at the discharge end. Minerals Engineering, 145, 106091. https://doi.org/10.1016/j.mineng.2019.106091
59. ISO 924:1989. Coal preparation plant. Principles and conventions for flowsheets. Available at: https://www.iso.org/standard/5340.html
60. DIN EN 1009-3. Maschinen für die mechanische Aufbereitung von Mineralien und ähnlichen festen Stoffen – Sicherheit – Teil 3: Spezifische Anforderungen für Brecher und Mühlen; Deutsche Fassung EN 1009-3:2020. Available at: https://www.din.de/de/mitwirken/normenausschuesse/nam/veroeffentlichungen/wdc-beuth:din21:316006092